Journal of Chemical&Engineering Data

pubs.acs.org/jced Article

Solid−Liquid Equilibrium and Binodal Curves for Aqueous Solutions of NH_3, NH_4HCO_3, MDEA, and K_2CO_3

Lucas Farias Falcchi Corrêa,* Kaj Thomsen, and Philip Loldrup Fosbøl*

Cite This: https://doi.org/10.1021/acs.jced.1c00144 Read Online

ACCESS | Metrics & More | Article Recommendations

ABSTRACT: Solid−liquid equilibrium (SLE) data were obtained at 0.1 MPa for binary, ternary, and quaternary aqueous solutions containing ammonia (NH_3), ammonium bicarbonate (NH_4HCO_3), methyl diethanolamine (MDEA), and potassium carbonate (K_2CO_3) using a modified Beckmann apparatus. The reproducibility of the experimental method was verified by measuring the SLE of aqueous solutions containing NH_3, K_2CO_3, or MDEA in a temperature range between 237 and 273 K. A total of 120 new data points were measured for MDEA−NH_3 and NH_4HCO_3−H_2O mixtures (250 to 305 K), and 23 new data points were obtained for MDEA−K_2CO_3−H_2O solutions (250 to 270 K). These measurements allow for an accurate estimation of water activity in such mixtures and provide insights on the limits of solid formation. The results indicate that the addition of MDEA increases the solubility of NH_4HCO_3, whereas a liquid−liquid split was observed when K_2CO_3 was added to aqueous MDEA. This opens the possibility of using it as a phase demixing solvent for carbon capture. Despite the extensive literature regarding mixed salt−amine solutions, liquid demixing in such systems has not been reported before. For this reason, the binodal curve for the MDEA−K_2CO_3−H_2O solution was measured at 293.15 K using the method of cloud point titration. These results assist the selection of operation parameters that avoid a liquid−liquid split in the process.

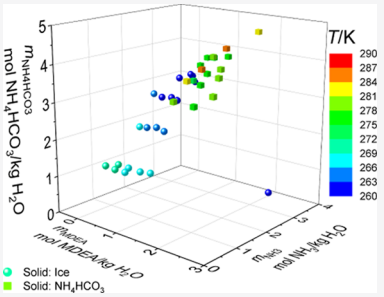

INTRODUCTION

According to IPCC, carbon capture and storage (CCS) is among the suite of technologies needed to limit global warming to 1.5 K by 2050.[1] CCS can be performed by absorption of carbon dioxide (CO_2), relying either on its physical solubility in the liquid phase or on its reactivity with such a solvent (chemical absorption). During the previous 5 years, approximately half of the operational or near-operational CCS units performed chemical absorption of CO_2.[2]

Aqueous amine solutions have been extensively tested for chemically absorbing CO_2 from gas streams.[3−5] Primary and secondary amine solutions readily react with dissolved CO_2 to form carbamate ions ($HNCOO^-$), while this reaction does not happen in solutions of tertiary and sterically hindered amines. In the last group, only bicarbonate and carbonate ions are formed at slower reaction rates.[6] On the other hand, the energy required to regenerate the CO_2-rich solvent is larger in the event of carbamate formation.[4] Moreover, the last group of amines is generally less susceptible to oxidative and thermal degradation than the first group.[7]

Ammonia (NH_3) and potassium carbonate (K_2CO_3) aqueous solutions are other mature alternatives for CO_2 absorption. The reaction between aqueous NH_3 and CO_2 has a similar mechanism to the reaction of primary amines and CO_2.[8] Nonetheless, simulation[9−13] and pilot plant[14,15] data suggest that the energy required to strip the loaded solvent in NH_3-based processes is lower than the value typically reported for units using monoethanolamine (MEA).[16] The main reason for such reduction is that CO_2 can be stripped at higher pressures when using aqueous NH_3, which reduces water vaporization and eliminates the energy it consumes.[8] On the other hand, the overall gas-phase mass-transfer coefficients of CO_2 are smaller in NH_3 than in MEA solutions, which may lead to larger separation columns.[8] Additionally, NH_3 is volatile and will inevitably slip to the gas phase, so additional separation steps must be considered to limit atmospheric emissions.

The K_2CO_3 aqueous solution is stable, non-toxic, and cheaper than most solvents for CO_2 absorption.[17] It can accommodate high operating pressures for CO_2 stripping, reducing the energy required for solvent regeneration, as in the NH_3-based capture. However, the slow rate of reaction may be prohibitive to the use of K_2CO_3 on itself. In this sense, several studies have suggested the use of promoters to enhance the rate of absorption in K_2CO_3 solutions.[17,18] Rate promoters are often categorized as inorganic oxyanions or amine-based organic compounds.[18] Their reaction mechanism with CO_2 can be generalized as (i) hydration of the promoter, rendering

Received: February 24, 2021
Accepted: June 21, 2021

it active; (ii) reaction with CO_2, forming an intermediate species; and (iii) deactivation of the promoter.[19] In this sense, NH_3 could be used as a rate promoter due to the fast-reacting carbamate formation.

A recent technology for CO_2 absorption combines both NH_3 and K_2CO_3 to obtain improved reaction rates and reduced emissions.[20] Bench-scale experiments were performed to study the capture efficiency of the new solvent[21] and the temperature dependence of the rate of absorption.[22] This new process could reduce the parasitic power demand by up to 50%, compared to state-of-the-art MEA-based processes; also, it uses 50−60% less water compared to conventional NH_3-based capture.[20] These improvements were supported by detailed process simulations performed in the framework of the extended UNIQUAC model.[16]

The extended UNIQUAC model[23] has been extensively used for simulations in CO_2 absorption systems. Interaction parameters between CO_2 and MEA,[24] *n*-methyldiethanolamine (MDEA),[24,25] piperazine,[26] or ammonia[27] have been obtained based on different types of phase equilibria (vapor pressure, vapor−liquid, and solid−liquid) and thermal (heat capacity and heat of absorption) data. ePC-SAFT has been used to model the mean ionic activity coefficient, the osmotic coefficient, the liquid−liquid equilibrium (LLE), and the density of alkali metal halides + organic solvent + water mixtures.[28−30] The model also provided an accurate prediction of the vapor−liquid equilibrium of sour gas and amine solvents using only parameters obtained from binary data.[31] COSMO-RS-based models have also been successfully used to predict the solid−liquid equilibrium (SLE) and LLE of salt + water/organic solvent systems.[28−30] COSMO-based models can perform fully predictive calculations and are excellent tools for solvent screening applications; however, models with adjustable binary parameters (such as the extended UNIQUAC and ePC-SAFT) tend to present smaller deviation from experimental measurements. In this respect, SLE data shed light on the limits of solid formation in a given mixture and provide reliable data for estimating water activity, which strongly affects the estimation of water loss in the stripping column.

The goal of this work is to investigate the thermodynamic properties of electrolyte solutions containing an organic solvent. The study was performed through the measurement of SLE data for aqueous mixtures containing MDEA and a strong (K_2CO_3) or weak (NH_3 or NH_4HCO_3) electrolyte. The data were obtained using a modified Beckmann apparatus[32] which has been extensively used for measurements of this nature.[33−36] A two-liquid-phase region was detected for MDEA−K_2CO_3 solutions at ambient temperature, so the boundary for liquid−liquid split was also investigated using the cloud point method.[37] To the best of our knowledge, this phenomenon has not been previously reported in the open literature regarding mixed salt−amine solutions. In this sense, this work not only contributes to further model development but also sheds light on a critical property of the investigated solvent.

EXPERIMENTAL SECTION

Chemicals. Table 1 lists the chemicals used in this work, which were used without further purification. Both K_2CO_3 and sodium chloride (NaCl) were dried at 373.15 K under vacuum (20 kPa) for at least 1 h immediately before use. The solutions were prepared using deionized water (0.2 μS cm^{-1}).

Table 1. Chemicals Used in This Work

chemical name	CAS	source	purity (mass fraction)	purification method
ammonium bicarbonate	1066-33-7	Honeywell	>0.99	none
ammonium hydroxide	1336-21-6	Sigma-Aldrich	0.28[a]	none
MDEA[b]	105-59-9	Sigma-Aldrich	>0.99	none
potassium carbonate	584-08-7	Sigma-Aldrich	>0.99	Vacuum drying
sodium chloride	7647-14-5	Sigma-Aldrich	>0.99	Vacuum drying

[a]Mass fraction of ammonia in water. [b]MDEA = *n*-methyldiethanolamine.

Methodology. The SLE data were measured using a modified Beckmann apparatus (Figure 1), which is described in detail elsewhere.[32] All samples were prepared in 50 mL flasks using deionized water and weighed using an analytical balance ($u(m_i)$ = 0.1 mg). The glass vial used for the measurements was filled with approximately 5 g of the aqueous solution using a disposable pipette and then inserted in an ethanol bath. The solution was stirred both using a magnetic bar sitting in the bottom of the vial and using a manual stirrer to ensure a homogeneous cooling of the sample. The temperature of the bath was kept between 5 and 10 K below the target temperature using an external refrigerated circulator (Julabo FP50). The temperature inside the vial was measured using a platinum resistance thermometer (Pt100 DIN 1/10), and it was recorded every 2 s throughout the experiment. The thermometer was calibrated against the freezing points of NaCl solutions[38] containing 0, 2.5, 5.0, 7.5, 10.0, 15.0, and 17.5% in weight of salt.

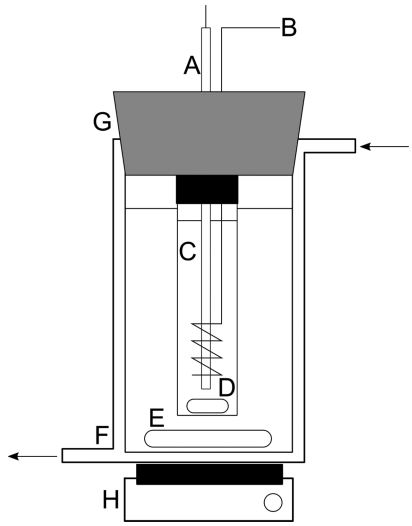

Figure 1. Experimental apparatus consisting of (A) resistance thermometer (Pt100), (B) manual stirrer, (C) sample flask, magnetic bars for (D) sample and (E) cooling media, (F) cooling jacket, (G) rubber stopper, and (H) magnetic stirrer.

Freezing point depression (FPD) data were measured by detecting the change of temperature in the vial due to the formation of ice crystals, whereas the precipitation of ammonium bicarbonate was visually determined as the heat evolved did not allow detection through a temperature change. In both cases, the first measurements are characterized by

https://doi.org/10.1021/acs.jced.1c00144
J. Chem. Eng. Data XXXX, XXX, XXX−XXX

Table 2. SLE Data for Aqueous Solutions Containing K_2CO_3, MDEA, or NH_3 at 0.1 MPa[a] (Solid Phase: Ice)

solute (i)	m_i,[b] mol/kg water	T,[c] K	$u_t(T)$,[d] K	solute (i)	m_i, mol/kg water	T, K	$u_t(T)$, K
K_2CO_3	0.050	272.90	0.05	K_2CO_3	4.760	239.51	0.04
K_2CO_3	0.050	272.80	0.02	K_2CO_3	4.949	237.13	0.10
K_2CO_3	0.100	272.65	0.03	K_2CO_3	4.949	237.73	0.23
K_2CO_3	0.257	272.31	0.06	MDEA	0.222	272.68	0.01
K_2CO_3	0.445	271.66	0.05	MDEA	0.446	272.25	0.03
K_2CO_3	0.450	271.77	0.02	MDEA	0.939	271.24	0.01
K_2CO_3	0.749	270.31	0.04	MDEA	1.485	270.06	0.01
K_2CO_3	0.996	269.11	0.02	MDEA	2.105	268.70	0.03
K_2CO_3	1.486	267.07	0.04	MDEA	2.805	267.05	0.01
K_2CO_3	2.051	263.65	0.02	MDEA	2.806	267.01	0.06
K_2CO_3	2.482	261.10	0.07	MDEA	3.600	264.65	0.02
K_2CO_3	2.988	257.46	0.08	NH_3	0.059	273.08	0.03
K_2CO_3	3.580	251.87	0.11	NH_3	0.523	272.13	0.01
K_2CO_3	3.580	252.15	0.12	NH_3	1.304	270.50	0.01
K_2CO_3	3.955	248.77	0.11	NH_3	2.656	267.50	0.02
K_2CO_3	4.290	245.18	0.16	NH_3	2.677	268.18	0.03
K_2CO_3	4.290	245.43	0.07	NH_3	3.873	264.42	0.02
K_2CO_3	4.600	241.83	0.28				

[a]Standard uncertainty for pressure, $u(p)$ = 1 kPa. [b]Standard uncertainty for molalities, $u(m_i)$ = 0.001 mol kg^{-1}. [c]Standard uncertainty for temperature, $u_c(T) = (u_{calibration}^2 + u_{repeatability}^2)^{1/2}$ = 0.05 K. [d]$u_t(T)$—standard deviation of five consecutive measurements.

excessive sub-cooling of the mixture due to the lack of nuclei for crystallization; therefore, they must be excluded from the analysis.[32] After a solid phase was detected, the vial was taken out from the cooling cell and manually stirred at ambient temperature. At the onset of disappearance of the solids in the solution, the vial was placed back in the cooling media. The experiment was finished when 5 consecutive measurements were obtained following this procedure, while the calibration with NaCl solutions required 10 consecutive measurements. If all solids in the vial were dissolved at a given point, an excessive sub-cooling would be noticed in the next measurement and the procedure would be restarted. The visual inspection of the solid phase introduces an additional uncertainty in the measurement of ammonium bicarbonate solubility, which is not considered when determining the reproducibility of the results using the standard deviation of consecutive measurements.

The limit of liquid−liquid split of aqueous MDEA-K_2CO_3 solutions was determined by the cloud point method.[37] Starting solutions containing K_2CO_3 were prepared in an analytical balance ($u(m_i)$ = 0.1 mg) and added to a glass jacketed reactor. The temperature in the reactor was kept at 293.15 K using an external refrigerated circulator (Julabo FP50). The liquid was mixed using a magnetic bar sitting in the bottom of the reactor. A rubber stopper with two openings was added to the top of the reactor. A platinum resistance thermometer (Pt100 DIN 1/10) was connected to one of such ports to record the temperature of the liquid phase; the other opening was used for adding MDEA step-wise. This injection was performed using a 20 mL syringe filled with the amine. The enthalpy change caused by the dilution of MDEA in the K_2CO_3 solution would increase the temperature of the mixture after the injection of amine; therefore, the system was allowed to reach thermal equilibrium after each addition. The solubility limit was established when the addition of one droplet of amine would cause the mixture to become turbid, indicating the presence of a small fraction of a second liquid phase. At this point, the solution was mixed for 10 min to check whether it would not become homogeneous again. The amount of added MDEA was determined by weighing the syringe both at the start and at the end of each experiment.

Equilibrium Calculation. The equilibrium between a solid salt ($A_\alpha B_\beta{\cdot}nH_2O$) and its corresponding aqueous solution can be represented by eq 1. It is known that the chemical potential of the salt will be equal to the sum of the chemical potentials of its constituents when equilibrium is reached. This criterion can be expressed based on standard chemical potentials and the deviation from such standard conditions, which is taken into consideration by the equilibrium constant of the salt ($K_{A_\alpha B_\beta{*}nH_2O}$), according to eq 2

$$A_\alpha B_\beta{\cdot}nH_2O_{(s)} \leftrightarrow \alpha A_{(aq)}^{\beta+} + \beta B_{(aq)}^{\alpha-} + nH_2O_{(l)} \quad (1)$$

$$K_{A_\alpha B_\beta{\cdot}nH_2O} = a_A^\alpha a_B^\beta a_{H_2O}^n \quad (2)$$

The temperature dependence of K can be derived from the Gibbs−Helmholtz equation leading to eq 3, in which Δa, Δb, and Δc are calculated from the individual coefficients of the heat capacity correlation given in eq 4. T_0 and T_Θ are reference temperatures that are arbitrarily set to 273.15 and 200.00 K, respectively.

$$R \ln K_T = R \ln K_{T_0} - \Delta H_{T_0}^0\left(\frac{1}{T} - \frac{1}{T_0}\right) + \Delta a\left(\ln\frac{T}{T_0} + \frac{T_0}{T} - 1\right) + 0.5\Delta b\left[\frac{(T-T_0)^2}{T}\right] + \frac{\Delta c}{T_\Theta}\left[\frac{(T-T_\Theta)}{T}\ln\left(\frac{T-T_\Theta}{T_0-T_\Theta}\right) - \ln\frac{T}{T_0}\right] \quad (3)$$

$$C_{p,i} = a_i + b_i T + \frac{c_i}{(T - T_\Theta)} \quad (4)$$

Provided that the constants for eq 4 and the standard state properties are known, an excess Gibbs energy model must be used to solve eq 2 and determine the equilibrium composition. This is done by introducing the solubility index (SI), which is the ratio between the product of activities ($a_A^\alpha a_B^\beta a_{H_2O}^n$) and the equilibrium constant ($K_{A_\alpha B_\beta{\cdot}nH_2O}$). The SI indicates whether the solution is saturated (SI = 1), supersaturated (SI > 1), or unsaturated (SI < 1).

https://doi.org/10.1021/acs.jced.1c00144
J. Chem. Eng. Data XXXX, XXX, XXX−XXX

In this work, equilibrium calculations were performed using the extended UNIQUAC model; the interested reader is referred to the original works[23,39] for further details on the derivation of the model and of the calculation procedure.

RESULTS AND DISCUSSION

SLE: K_2CO_3–H_2O, MDEA–H_2O, and NH_3–H_2O. Table 2 shows the SLE data for binary aqueous solutions of K_2CO_3, MDEA, and NH_3 which were measured to validate the experimental procedure. A good agreement is observed when comparing such data to publications available in the open literature, as shown in Figures 2–4. The maximum standard deviation of the measured temperatures was $u(T)$ = 0.28 K. The repeatability of the measurements is expectedly lower when working with increasing solute concentration (i.e., lower temperatures) due to a less efficient mixing of the sample resulting from higher viscosities.[32] The data for aqueous MDEA solutions (Figure 3) agree with most of the experimental data and support the evidence that at least one of the data sets available might be inaccurate. The statement that only ice is formed during the experiment is supported both by the temperature profile of the experiment, which showed the typical behavior for ice formation,[32] and by SLE compositions determined using the extended UNIQUAC model.[23]

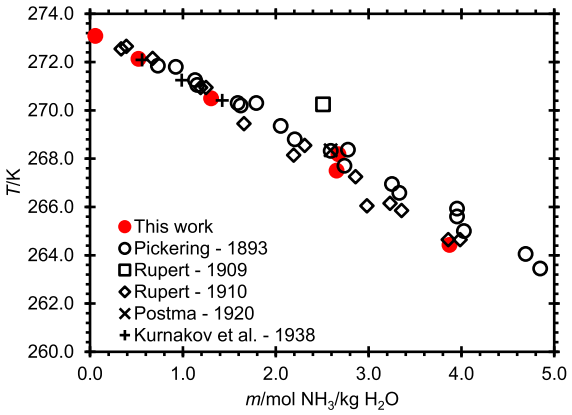

Figure 2. SLE data for aqueous ammonia solutions.[40−44]

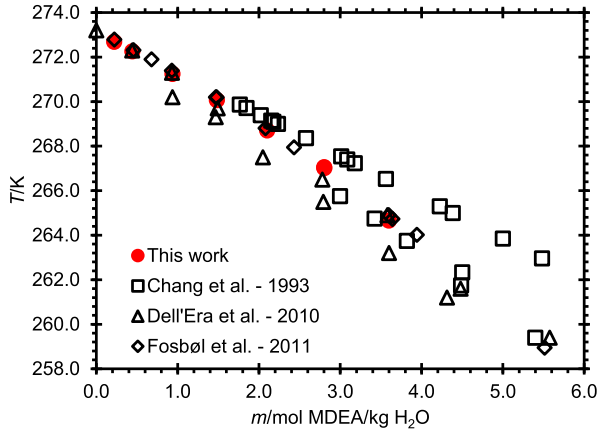

Figure 3. SLE data for aqueous MDEA solutions.[32,45,46]

SLE: MDEA–NH_3, NH_4HCO_3–H_2O, and MDEA–NH_3–NH_4HCO_3–H_2O. Tables 3–6 show the measurements for ternary and quaternary aqueous solutions containing MDEA, NH_3, and/or NH_4HCO_3. The highest standard deviation of the measured temperature was $u(T)$ = 0.12 K for FPD data, and $u(T)$ = 0.62 K for NH_4HCO_3 solubility measurements. It is known[34] that solubility experiments generally result in a lower repeatability compared to FPD measurements since they rely on visual detection of the solubility limit, while FPD measurements rely directly on the temperature profile. Figure 5 shows a selection of data (Tables 4 and 5) obtained in this work, compared to the SLE diagram for aqueous NH_4HCO_3 determined by the extended UNIQUAC model. The graph does not show model calculations for the mixtures containing NH_4HCO_3 because there are no sufficient phase equilibrium data available to estimate the interactions between NH_4^+ and MDEA/MDEAH$^+$.

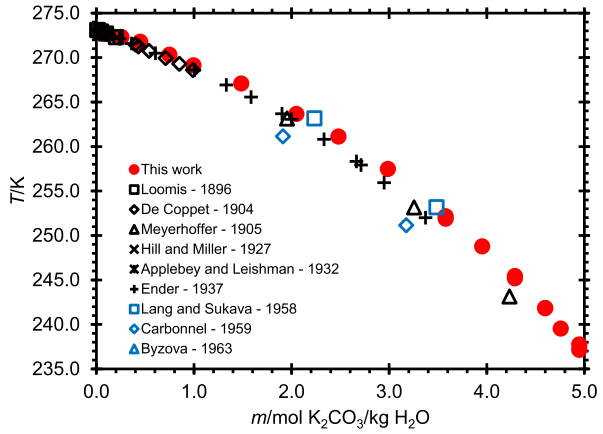

Figure 4. SLE data for aqueous potassium carbonate solutions.[47−55]

Table 3. SLE Data for Aqueous Solutions Containing MDEA and NH_3 at 0.1 MPa[a]

m_{MDEA},[b] mol/kg water	m_{NH_3}, mol/kg water	T,[c] K	$u_t(T)$,[d] K	solid phase
0.959	1.462	267.71	0.03	ice
0.980	2.972	264.28	0.02	ice
1.008	4.584	260.10	0.04	ice
2.154	1.635	264.55	0.04	ice
2.216	3.365	260.15	0.05	ice
2.292	5.193	254.72	0.07	ice
3.707	1.870	259.56	0.01	ice
3.833	3.883	253.29	0.04	ice

[a]Standard uncertainty for pressure, $u(p)$ = 1 kPa. [b]Standard uncertainty for molalities, $u(m_i)$ = 0.001 mol kg^{-1}. [c]Standard uncertainty for temperature, $u_c(T) = (u_{calibration}^2 + u_{repeatability}^2)^{1/2}$ = 0.05 K. [d]$u_t(T)$—standard deviation of five consecutive measurements.

The results clearly show an increase in the solubility of NH_4HCO_3 as more MDEA is added to the aqueous solution. At approximately 290 K, for example, the saturation of NH_4HCO_3 (in moles NH_4HCO_3 per kilogram of water) in the 2.0 mol MDEA/kg H_2O solution is ca. 50% higher than the saturation in pure water. This could be justified by an increase in the solution pH due to the addition of MDEA (pK_a = 8.6 at 298.15 K),[66,67] which would reduce the concentration of bicarbonate ions. In practice, this phenomenon implies that the addition of MDEA to the solvent may prevent precipitation of NH_4HCO_3 at higher CO_2 concentrations when using mixed solvents containing both NH_3 and MDEA.

In these experiments, as in the validation systems, the solid phase was determined both by analyzing the temperature

https://doi.org/10.1021/acs.jced.1c00144
J. Chem. Eng. Data XXXX, XXX, XXX−XXX

Table 4. SLE Data for Aqueous Solutions Containing MDEA and NH_4HCO_3 at 0.1 MPa[a] (Solid Phase: Ice)

m_{MDEA},[b] mol/kg water	$m_{NH_4HCO_3}$, mol/kg water	T,[c] K	$u_t(T)$,[d] K	m_{MDEA} mol/kg water	$m_{NH_4HCO_3}$ mol/kg water	T, K	$u_t(T)$, K
0.460	0.506	271.51	0.05	1.499	2.250	264.74	0.02
0.491	0.988	270.02	0.03	1.504	1.003	267.83	0.06
0.501	0.759	270.28	0.03	1.511	1.366	266.88	0.05
0.501	1.566	268.26	0.01	1.923	0.948	266.57	0.07
0.501	1.746	267.87	0.02	1.973	1.322	265.73	0.05
0.501[e]	*1.856*	*272.07*	*0.07*	1.996	0.547	267.52	0.03
0.521	1.317	268.98	0.03	2.000	0.750	266.78	0.02
0.978	0.504	269.77	0.06	2.000	1.508	264.97	0.04
1.001	0.749	269.28	0.02	2.000	1.800	264.38	0.01
1.001	1.505	267.48	0.02	2.000	2.002	263.86	0.01
1.001	1.759	266.99	0.01	2.000	2.251	263.35	0.03
1.001	1.850	266.63	0.02	2.000	2.509	262.87	0.01
1.001	2.001	266.32	0.03	2.975	1.020	263.45	0.10
1.001	2.132	266.17	0.01	2.978	1.318	262.80	0.04
1.005	0.989	268.91	0.12	2.994	0.523	265.27	0.05
1.033	1.403	267.63	0.06	3.971	1.418	259.34	0.06
1.498	0.513	268.86	0.06	3.978	0.475	261.98	0.03
1.499	0.743	268.11	0.02	3.990	0.984	260.48	0.10
1.499	1.510	266.32	0.01	4.935	0.501	258.72	0.04
1.499	1.752	265.67	0.03	4.989	1.336	256.11	0.09
1.499	1.864	265.52	0.01	5.004	1.024	256.68	0.06
1.499	1.998	265.25	0.01	5.971	0.490	254.99	0.04
1.499	2.151	264.90	0.02				

[a]Standard uncertainty for pressure, $u(p)$ = 1 kPa. [b]Standard uncertainty for molalities, $u(m_i)$ = 0.001 mol kg^{-1}. [c]Standard uncertainty for temperature, $u_c(T) = (u_{calibration}^2 + u_{repeatability}^2)^{1/2}$ = 0.05 K. [d]$u_t(T)$—standard deviation of five consecutive measurements. [e]Meta-stable points—both ice and NH_4HCO_3.

Table 5. SLE Data for Aqueous Solutions Containing MDEA and NH_4HCO_3 at 0.1 MPa[a] (Solid Phase: NH_4HCO_3)

m_{MDEA},[b] mol/kg water	$m_{NH_4HCO_3}$, mol/kg water	T,[c] K	$u_t(T)$,[d] K	m_{MDEA}, mol/kg water	$m_{NH_4HCO_3}$, mol/kg water	T, K	$u_t(T)$, K
0.496	1.917	272.22	0.13	2.000	3.246	280.93	0.24
0.497	2.274	280.03	0.11	2.000	3.751	288.54	0.12
0.501	2.500	284.72	0.28	2.000	4.007	292.28	0.26
0.501	3.004	292.39	0.62	2.000	4.247	296.20	0.19
0.517	2.320	280.49	0.11	2.000	4.503	298.93	0.15
1.001	2.524	278.07	0.30	2.000	4.747	302.81	0.57
1.001	3.026	286.90	0.04	2.000	5.002	304.44	0.38
1.036	2.449	275.42	0.17	2.023	2.983	274.54	0.18
1.477	2.562	274.96	0.09	2.710	3.579	280.43	0.23
1.489	2.824	277.46	0.13	2.971	3.350	274.02	0.11
1.499	2.503	271.55	0.16	3.372	3.686	277.71	0.17
1.499	3.028	280.98	0.26	4.013	3.419	270.85	0.19
1.566	2.697	273.27	0.11	4.605	3.509	273.17	0.08
2.000	2.753	271.59	0.09	5.092	3.737	273.35	0.23
2.000	3.120	278.81	0.15				

[a]Standard uncertainty for pressure, $u(p)$ = 1 kPa. [b]Standard uncertainty for molalities, $u(m_i)$ = 0.001 mol kg^{-1}. [c]Standard uncertainty for temperature, $u_c(T) = (u_{calibration}^2 + u_{repeatability}^2)^{1/2}$ = 0.05 K. [d]$u_t(T)$—standard deviation of five consecutive measurements.

profile during the experiment and by predicting the solids which might be formed at a given concentration. In this case, however, the model could not give a reasonable estimate as the parameters for the MDEA−NH_3 pair were not available yet. A meta-stable region with two solid phases was observed for one of the samples (highlighted in Table 3). The presence of two distinct phases was confirmed by a second experiment using the same stock solution. In both cases, the pieces of evidence of two separate solids were both a temperature increase during crystallization, indicating ice formation, and a second solid phase with a higher melting point.

SLE and Binodal Curve: MDEA−K_2CO_3−H_2O. Table 7 shows the measurements for ternary aqueous solutions containing MDEA and K_2CO_3. The highest standard deviation of the measured temperature was $u(T)$ = 0.19 K. The number of experiments was limited due to liquid−liquid split, which was observed both when mixing the components at ambient temperature and during some of the SLE measurements. The binodal curve at 293.15 K was measured through cloud point titration (Table 8) and might provide a starting point for future studies on the LLE of such mixtures. The results are presented together with the solubility of potassium carbonate sesquihydrate (K_2CO_3·1.5H_2O) at 293.15 K calculated by the

https://doi.org/10.1021/acs.jced.1c00144
J. Chem. Eng. Data XXXX, XXX, XXX−XXX

Table 6. SLE Data for Aqueous Solutions Containing MDEA, NH_3, and NH_4HCO_3 at 0.1 MPa[a]

solid phase: ice					solid phase: NH_4HCO_3				
m_{MDEA},[b] mol/kg water	m_{NH_3}, mol/kg water	$m_{NH_4HCO_3}$, mol/kg water	T,[c] K	$u_t(T)$,[d] K	m_{MDEA}, mol/kg water	m_{NH_3}, mol/kg water	$m_{NH_4HCO_3}$, mol/kg water	T, K	$u_t(T)$, K
0.126	3.681	2.864	260.92	0.04	1.128	2.713	3.965	276.37	0.18
0.145	3.545	2.966	261.07	0.04	1.205	2.370	3.843	277.68	0.16
0.218	2.143	2.900	263.61	0.05	1.295	2.701	3.997	275.23	0.18
0.247	3.428	3.126	260.25	0.04	1.301	2.003	3.533	274.06	0.11
0.258	1.625	2.116	266.18	0.06	1.491	2.392	4.119	280.91	0.44
0.274	0.937	1.269	269.10	0.06	1.528	1.493	3.681	281.05	0.19
0.289	3.295	3.213	260.58	0.04	1.621	2.709	4.087	275.13	0.10
0.301	0.530	1.378	269.47	0.05	1.633	1.991	3.786	277.07	0.08
0.441	2.122	2.861	262.81	0.05	1.725	0.822	3.364	279.81	0.25
0.474	1.593	2.161	265.10	0.05	1.802	2.371	4.395	284.09	0.29
0.536	0.935	1.258	268.02	0.12	1.831	1.504	3.645	277.65	0.15
0.553	2.556	3.322	260.50	0.06	1.842	1.521	4.040	285.26	0.21
0.557	0.513	1.364	269.97	0.03	1.942	1.990	3.964	278.29	0.14
0.665	2.144	2.899	261.83	0.10	2.099	3.013	4.768	282.20	0.17
0.702	1.610	2.220	264.11	0.03	2.155	0.850	3.338	277.63	0.19
0.799	0.523	1.364	267.66	0.03	2.239	1.493	3.912	280.91	0.20
0.815	0.953	1.237	267.07	0.06	2.539	0.892	3.666	278.81	0.22
0.816	2.131	2.858	261.60	0.04					
0.872	1.634	2.152	263.66	0.07					
1.059	0.965	1.276	266.42	0.06					
2.363	3.097	0.439	260.11	0.07					

[a]Standard uncertainty for pressure, $u(p)$ = 1 kPa. [b]Standard uncertainty for molalities, $u(m_i)$ = 0.001 mol kg^{-1}. [c]Standard uncertainty for temperature, $u_c(T) = (u_{calibration}^2 + u_{repeatability}^2)^{1/2}$ = 0.05 K. [d]$u_t(T)$—standard deviation of five consecutive measurements.

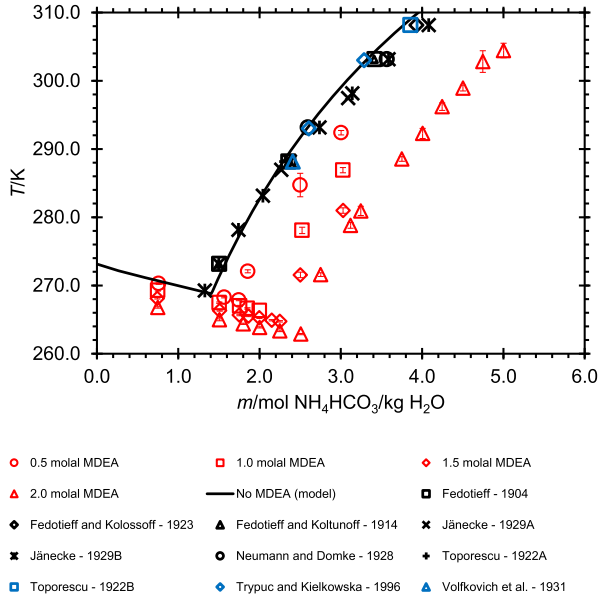

Figure 5. Selected SLE data for aqueous solutions containing MDEA, NH_3, and NH_4HCO_3 compared to the phase boundary of aqueous NH_4HCO_3 from the literature[56−65] and determined by the extended UNIQUAC model.

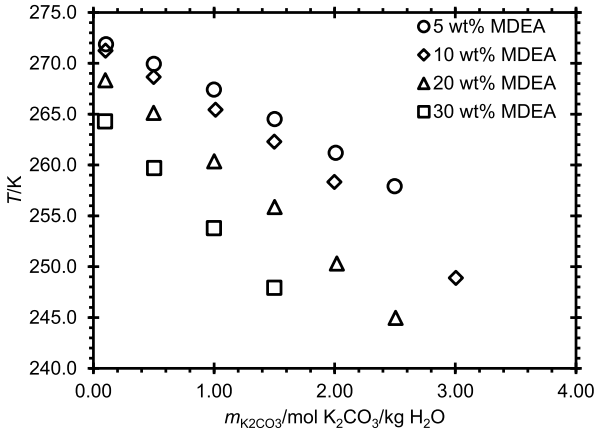

Figure 6. SLE data for aqueous solutions containing MDEA and K_2CO_3.

extended UNIQUAC model (Figure 7). This calculation was carried out considering no interactions between K^+ and MDEA/$MDEAH^+$ since the model parameters are still not available for such species. No phase splitting was observed during the SLE measurements reported previously, and a critical analysis of Figures 6 and 7 shows that such experiments were made at a one-liquid-phase region.

K_2CO_3 has been previously identified as an efficient salting-out agent for aqueous solutions of alcohols, acetone, and aprotic solvents (both polar and apolar).[68,69] A simple explanation for this phenomenon is that the addition of an electrolyte changes the aqueous solvation shell and enhances the hydrophobic effect; this will lead the organic solute (in this case, MDEA) to aggregate up to the point of a phase split.[68] However, the specific mechanism for salting effects is probably much more complex and it is still open to debate, which is beyond the scope of this paper.[68,70,71] Nonetheless, the literature in the field suggests some general trends regarding the magnitude of specific ion effects. In most cases, such effects will increase for solutes that possess higher polarizability, a larger molecular size, and lower polarity.[68] Regardless of these observations, no reports on the LLE of aqueous MDEA−K_2CO_3 are reported in the open literature. While this effect

https://doi.org/10.1021/acs.jced.1c00144
J. Chem. Eng. Data XXXX, XXX, XXX−XXX

Table 7. SLE Data for Aqueous Solutions Containing MDEA and K_2CO_3 at 0.1 MPa[a] (Solid Phase: Ice)

$m_{K_2CO_3}$,[b] mol/kg water	m_{MDEA}, mol/kg water	T,[c] K	$u_t(T)$,[d] K	$m_{K_2CO_3}$, mol/kg water	m_{MDEA}, mol/kg water	T, K	$u_t(T)$, K
0.098	3.647	264.27	0.06	1.499	1.130	262.29	0.09
0.099	2.127	268.34	0.01	1.500	4.344	247.92	0.16
0.101	0.948	271.25	0.02	1.502	2.530	255.87	0.07
0.106	0.452	271.87	0.02	1.503	0.532	264.50	0.02
0.499	2.245	265.13	0.11	1.998	1.189	258.34	0.03
0.500	0.996	268.66	0.03	2.009	0.562	261.19	0.02
0.501	0.471	269.93	0.01	2.018	2.683	250.31	0.06
0.504	3.850	259.68	0.05	2.493	1.252	254.34	0.19
1.000	0.503	267.41	0.01	2.498	0.596	257.90	0.07
1.000	4.095	253.78	0.12	2.505	2.822	244.97	0.06
1.001	2.386	260.36	0.05	3.005	1.321	248.90	0.17
1.012	1.067	265.43	0.08				

[a]Standard uncertainty for pressure, $u(p)$ = 1 kPa. [b]Standard uncertainty for molalities, $u(m_i)$ = 0.001 mol kg^{-1}. [c]Standard uncertainty for temperature, $u_c(T) = (u_{calibration}^2 + u_{repeatability}^2)^{1/2}$ = 0.05 K. [d]$u_t(T)$—standard deviation of five consecutive measurements.

Table 8. Binodal Curve of Aqueous Solutions Containing MDEA and K_2CO_3 at T = 293.15 K[a] and 0.1 MPa[b]

$w_{K_2CO_3}$[c]	w_{MDEA}	w_{H_2O}
0.087	0.412	0.501
0.107	0.369	0.524
0.135	0.316	0.549
0.175	0.252	0.573
0.203	0.208	0.589
0.241	0.151	0.608
0.292	0.088	0.620
0.350	0.042	0.608

[a]Standard uncertainty for pressure, $u(p)$ = 1 kPa. [b]Standard uncertainty for temperature, $u_c(T) = (u_{calibration}^2 + u_{repeatability}^2)^{1/2}$ = 0.05 K. [c]Standard uncertainty for weight fraction, $u(w_i)$ = 0.001.

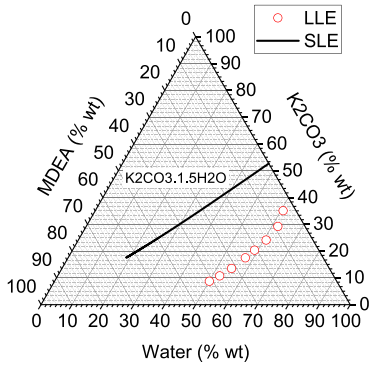

Figure 7. Binodal curve of aqueous solutions containing MDEA and K_2CO_3 at T = 293.15 K and solubility limit of potassium carbonate sesquihydrate estimated by the extended UNIQUAC model at the same temperature.

may be detrimental for normal operation of a CCS unit, it indicates that the MDEA–K_2CO_3 solution is a candidate for phase demixing solvents, which are of current interest for carbon capture technologies.[35] The current parameterization of the extended UNIQUAC model does not lead to a solution with two coexisting liquid phases in the region where this phenomenon was observed experimentally, as shown in Figure 7. This indicates the need of further experimental measurements to enhance the model, making it suitable for the prediction of liquid–liquid demixing in such solvents, and to understand the influence of different inorganic salts in aqueous amine solutions.

CONCLUSIONS

This work presents SLE data for binary, ternary, and quaternary mixtures containing ammonia (NH_3), ammonium bicarbonate (NH_4HCO_3), methyl diethanolamine (MDEA), and potassium carbonate (K_2CO_3) using a modified Beckmann apparatus. Binary data were obtained to validate the experimental procedure; the results agree with the extensive literature data accordingly. A total of 120 new data points were measured for MDEA–NH_3 and NH_4HCO_3–H_2O mixtures; the results show that the addition of MDEA leads to a higher solubility of NH_4HCO_3 per kilogram of water. A practical implication of these results is that the risk of precipitation of NH_4HCO_3 is lower when MDEA is present in the system. A total of 23 new data points were obtained for MDEA–K_2CO_3–H_2O solutions. The number of experiments was limited due to a liquid–liquid split at high concentrations of the salt, clearly indicating a salting-out effect. This phenomenon has not been previously published for mixed salt-amine systems, so the binodal curve was measured at 293.15 K to establish the limit of phase split. The liquid demixing limits the operation of CCS units to a low concentration of the salt; however, it indicates a potential use of the MDEA–K_2CO_3–H_2O solution as a phase demixing solvent.

AUTHOR INFORMATION

Corresponding Authors

Lucas Farias Falcchi Corrêa – *Department of Chemical and Biochemical Engineering, Center for Energy Resources Engineering (CERE), Technical University of Denmark, DK-2800 Kongens Lyngby, Denmark;* orcid.org/0000-0002-9134-9632; Email: lufco@kt.dtu.dk

Philip Loldrup Fosbøl – *Department of Chemical and Biochemical Engineering, Center for Energy Resources Engineering (CERE), Technical University of Denmark, DK-2800 Kongens Lyngby, Denmark;* orcid.org/0000-0003-1067-2348; Phone: +45 4525 2868; Email: plf@kt.dtu.dk

Author

Kaj Thomsen – *Department of Chemical and Biochemical Engineering, Center for Energy Resources Engineering (CERE), Technical University of Denmark, DK-2800*

https://doi.org/10.1021/acs.jced.1c00144
J. Chem. Eng. Data XXXX, XXX, XXX–XXX

Kongens Lyngby, Denmark; orcid.org/0000-0003-1373-1630

Complete contact information is available at: https://pubs.acs.org/10.1021/acs.jced.1c00144

Notes

The authors declare no competing financial interest.

■ ACKNOWLEDGMENTS

The authors thank SRI International and the Technical University of Denmark for the financial support (SRI sub award no PO27088) and Jesper Frandsen, who measured some of the SLE data presented in this work as part of his studies.

■ REFERENCES

(1) IPCC. *In Global Warming of 1.5 °C. An IPCC Special Report on the impacts of global warming of 1.5 °C above pre-industrial levels and related global greenhouse gas emission pathways, in the context of strengthening the global response to the threat of climate change, sustainable development, and efforts to eradicate poverty*; Masson-Delmotte, V.; et al., Eds, 2018, in press.

(2) Mumford, K. A.; Wu, Y.; Smith, K. H.; Stevens, G. W. Review of Solvent Based Carbon-Dioxide Capture Technologies. *Front. Chem. Sci. Eng.* **2015**, *9*, 125−141.

(3) Svendsen, H. F.; Hessen, E. T.; Mejdell, T. Carbon Dioxide Capture by Absorption, Challenges and Possibilities. *Chem. Eng. J.* **2011**, *171*, 718−724.

(4) Rochelle, G. T. In *Absorption-Based Post-Combustion Capture of Carbon Dioxide*; Feron, P. H. M., Ed.; Elsevier, 2016; pp 35−67.

(5) Sreedhar, I.; Nahar, T.; Venugopal, A.; Srinivas, B. Carbon Capture by Absorption - Path Covered and Ahead. *Renewable Sustainable Energy Rev.* **2017**, *76*, 1080−1107.

(6) Puxty, G.; Maeder, M. In *Absorption-Based Post-Combustion Capture of Carbon Dioxide*; Feron, P. H. M., Ed.; Elsevier, 2016; pp 13−33.

(7) Reynolds, A. J.; Verheyen, T. V.; Meuleman, E. In *Absorption-Based Post-Combustion Capture of Carbon Dioxide*; Feron, P. H. M., Ed.; Elsevier, 2016; pp 399−423.

(8) Yu, H.; Feron, P. H. M. In *Absorption-Based Post-Combustion Capture of Carbon Dioxide*; Feron, P. H. M., Ed.; Elsevier, 2016; pp 283−301.

(9) Darde, V.; Thomsen, K.; van Well, W. J. M.; Stenby, E. H. Chilled Ammonia Process for CO_2 Capture. *Energy Procedia* **2009**, *1*, 1035−1042.

(10) Mathias, P. M.; Reddy, S.; O'Connell, J. P. Quantitative Evaluation of the Chilled-Ammonia Process for CO_2 Capture Using Thermodynamics Analysis and Process Simulation. *Int. J. Greenhouse Gas Control* **2010**, *4*, 174−179.

(11) Valenti, G.; Bonalumi, D.; Macchi, E. A Parametric Investigation of the Chilled Ammonia Process from Energy and Economic Perspectives. *Fuel* **2012**, *101*, 74−83.

(12) Darde, V.; Maribo-Mogensen, B.; van Well, W. J. M.; Stenby, E. H.; Thomsen, K. Process Simulation of CO_2 Capture with Aqueous Ammonia Using the Extended UNIQUAC Model. *Int. J. Greenhouse Gas Control* **2012**, *10*, 74−87.

(13) Jilvero, H.; Normann, F.; Andersson, K.; Johnsson, F. Heat Requirement for Regeneration of Aqueous Ammonia in Post-Combustion Carbon Dioxide Capture. *Int. J. Greenhouse Gas Control* **2012**, *11*, 181−187.

(14) Yu, H.; Morgan, S.; Allport, A.; Cottrell, A.; Do, T.; McGregor, J.; Wardhaugh, L.; Feron, P. Results from Trialling Aqueous NH_3 Based Post-Combustion Capture in a Pilot Plant at Munmorah Power Station: Absorption. *Chem. Eng. Res. Des.* **2011**, *89*, 1204−1215.

(15) Han, K.; Ahn, C. K.; Lee, M. S. Performance of an Ammonia-based CO_2 Capture Pilot Facility in Iron and Steel Industry. *Int. J. Greenhouse Gas Control* **2014**, *27*, 239−246.

(16) Jayaweera, I.; Jayaweera, P.; Kundu, P.; Anderko, A.; Thomsen, K.; Valenti, G.; Bonalumi, D.; Lillia, S. Results from Process Modeling of the Mixed-salt Technology for CO_2 Capture from Post-Combustion-Related Applications. *Energy Procedia* **2017**, *114*, 771−780.

(17) Borhani, T. N. G.; Azarpour, A.; Akbari, V.; Wan Alwi, S. R.; Manan, Z. A. CO_2 Capture with Potassium Carbonate Solutions: A State-of-the-Art Review. *Int. J. Greenhouse Gas Control* **2015**, *41*, 142−162.

(18) Smith, K. H.; Nicholas, N. J.; Stevens, G. W. In *Absorption-Based Post-Combustion Capture of Carbon Dioxide*; Feron, P. H. M., Ed.; Elsevier, 2016; pp 145−166. DOI: 10.1016/b978-0-08-100514-9.00007-x

(19) Astarita, G.; Savage, D. W.; Longo, J. M. Promotion of CO_2 Mass Transfer in Carbonate Solutions. *Chem. Eng. Sci.* **1981**, *36*, 581−588.

(20) Jayaweera, I.; Jayaweera, P.; Elmore, R.; Bao, J.; Bhamidi, S. Update on Mixed-Salt Technology Development for CO_2 Capture from Post-Combustion Power Stations. *Energy Procedia* **2014**, *63*, 640−650.

(21) Jayaweera, I.; Jayaweera, P.; Yamasaki, Y.; Elmore, R. In *Absorption-Based Post-Combustion Capture of Carbon Dioxide*; Feron, P. H. M., Ed.; Elsevier, 2016; pp 168−200.

(22) Lillia, S.; Bonalumi, D.; Fosbøl, P. L.; Thomsen, K.; Jayaweera, I.; Valenti, G. Thermodynamic and Kinetic Properties of NH_3-K_2CO_3-CO_2-H_2O System for Carbon Capture Applications. *Int. J. Greenhouse Gas Control* **2019**, *85*, 121−131.

(23) Thomsen, K.; Rasmussen, P. Modeling of Vapor-Liquid-Solid Equilibrium in Gas-Aqueous Electrolyte Systems. *Chem. Eng. Sci.* **1999**, *54*, 1787−1802.

(24) Faramarzi, L.; Kontogeorgis, G. M.; Thomsen, K.; Stenby, E. H. Extended UNIQUAC Model for Thermodynamic Modeling of CO_2 Absorption in Aqueous Alkanolamine Solutions. *Fluid Phase Equilib.* **2009**, *282*, 121−132.

(25) Sadegh, N.; Stenby, E. H.; Thomsen, K. Thermodynamic modeling of CO_2 absorption in aqueous N-Methyldiethanolamine using Extended UNIQUAC model. *Fuel* **2015**, *144*, 295−306.

(26) Fosbøl, P. L.; Maribo-Mogensen, B.; Thomsen, K. Solids Modelling and Capture Simulation of Piperazine in Potassium Solvents. *Energy Procedia* **2013**, *37*, 844−859.

(27) Darde, V.; van Well, W. J. M.; Stenby, E. H.; Thomsen, K. Modeling of Carbon Dioxide Absorption by Aqueous Ammonia Solutions Using the Extended UNIQUAC Model. *Ind. Eng. Chem. Res.* **2010**, *49*, 12663−12674.

(28) Held, C. Thermodynamic g^E Models and Equations of State for Electrolytes in a Water-Poor Medium: A Review. *J. Chem. Eng. Data* **2020**, *65*, 5073−5082.

(29) Mohammad, S.; Held, C.; Altuntepe, E.; Köse, T.; Gerlach, T.; Smirnova, I.; Sadowski, G. Salt Influence on MIBK/Water Liquid-Liquid Equilibrium: Measuring and Modeling with ePC-SAFT and COSMO-RS. *Fluid Phase Equilib.* **2016**, *416*, 83−93.

(30) Ascani, M.; Held, C. Prediction of Salting-out in Liquid-Liquid Two-Phase Systems with ePC-SAFT: Effect of the Born Term and of a Concentration-Dependent Dielectric Constant. *Z. Anorg. Allg. Chem.* **2021**, *647*, 1305−1314.

(31) Bülow, M.; Gerek Ince, N.; Hirohama, S.; Sadowski, G.; Held, C. Predicting Vapor-Liquid Equilibria for Sour-Gas Absorption in Aqueous Mixtures of Chemical and Physical Solvents or Ionic Liquids with ePC-SAFT. *Ind. Eng. Chem. Res.* **2021**, *60*, 6327−6336.

(32) Fosbøl, P. L.; Pedersen, M. G.; Thomsen, K. Freezing Point Depressions of Aqueous MEA, MDEA, and MDEA-MDEA Measured with a New Apparatus. *J. Chem. Eng. Data* **2011**, *56*, 995−1000.

(33) Liu, Y.; Meyer, A. S.; Nie, Y.; Zhang, S.; Zhao, Y.; Fosbøl, P. L.; Thomsen, K. Freezing Point Determination of Water-Ionic Liquid Mixtures. *J. Chem. Eng. Data* **2017**, *62*, 2374−2383.

(34) Fosbøl, P. L.; Neerup, R.; Arshad, M. W.; Tecle, Z.; Thomsen, K. Aqueous Solubility of Piperazine and 2-Amino-2-methyl-1-propanol plus Their Mixtures Using an Improved Freezing-Point Depression Method. *J. Chem. Eng. Data* **2011**, *56*, 5088−5093.

(35) Arshad, M. W.; Fosbøl, P. L.; von Solms, N.; Thomsen, K. Freezing Point Depressions of Phase Change CO_2 Solvents. *J. Chem. Eng. Data* **2013**, *58*, 1918−1926.
(36) Neerup, R.; Ståhl, K.; Fosbøl, P. L. Solid Solubility in the Aqueous 2-Amino-2-methyl-propanol (AMP) Plus Piperazine (PZ) System. *J. Chem. Eng. Data* **2019**, *64*, 2423−2428.
(37) Sørensen, J. M.; Magnussen, T.; Rasmussen, P.; Fredenslund, A. Liquid-Liquid Equilibrium Data: Their Retrieval, Correlation and Prediction Part I: Retrieval. *Fluid Phase Equilib.* **1979**, *2*, 297−309.
(38) Clarke, E. C. W.; Glew, D. N. Evaluation of the Thermodynamic Functions for Aqueous Sodium Chloride from Equilibrium and Calorimetric Measurements below 154 °C. *J. Phys. Chem. Ref. Data* **1985**, *14*, 489−610.
(39) Thomsen, K. Aqueous Electrolytes Model Parameters and Process Simulation. Ph.D. Thesis, Technical University of Denmark (DTU), Kgs. Lyngby, 1997.
(40) Pickering, S. U. X.-The hydrate theory of solutions. Some compounds of the alkyl-amines and ammonia with water. *J. Chem. Soc.* **1893**, *63*, 141.
(41) Rupert, F. F. The Solid Hydrates of Ammonia. *J. Am. Chem. Soc.* **1909**, *31*, 866−868.
(42) Rupert, F. F. The Solid Hydrates of Ammonia II. *J. Am. Chem. Soc.* **1910**, *32*, 748−749.
(43) Postma, S. Le Systéme Ammoniaque—Eau. *Recl. Trav. Chim. Pays-Bas* **1920**, *39*, 515−536.
(44) Kurnakov, N. S.; Ravich, M. I.; Troitskaya, N. V. The Ice Fields of the Ternary Systems: Base-Acid-Water. Formation of Phosphates, Chromates and Borates. *Izv. Sektora Fiz.-Khim. Anal., Akad. Nauk SSSR* **1938**, *10*, 275−304.
(45) Chang, H. T.; Posey, M.; Rochelle, G. T. Thermodynamics of Alkanolamine-Water Solutions from Freezing Point Measurements. *Ind. Eng. Chem. Res.* **1993**, *32*, 2324−2335.
(46) Dell'Era, C.; Uusi-Kyyny, P.; Tautama, E.-L.; Pakkanen, M.; Alopaeus, V. Thermodynamics of Aqueous Solutions of Methyldiethanolamine and Diisopropanolamine. *Fluid Phase Equilib.* **2010**, *299*, 51−59.
(47) Loomis, E. H. On the Freezing-Points of Dilute Aqueous Solutions. *Phys. Rev.* **1896**, *3*, 270−292.
(48) de Coppet, L. C. On the Molecular Depression of the Freezing-point of Water Produced by Some Very Concentrated Saline Solutions. *J. Phys. Chem.* **1904**, *8*, 531−538.
(49) Meyerhoffer, W. Über reziproke Salzpaare. IV. Ein Problem der Affinitätslehre. *Z. Phys. Chem.* **1905**, *53*, 513−603.
(50) Hill, A. E.; Miller, F. W. Ternary Systems IV. Potassium Carbonate, Sodium Carbonate and Water. *J. Am. Chem. Soc.* **1927**, *49*, 669−686.
(51) Applebey, M. P.; Leishman, M. A. The System Potassium Carbonate - Ammonia - Water. *J. Chem. Soc.* **1932**, *0*, 1603−1608.
(52) Ender, F. Zur Individualität des Osmotischen Verhaltens der Alkalicarbonate. *Z. Elektrochem. Angew. Phys. Chem.* **1937**, *43*, 234−238.
(53) Lang, A. A.; Sukava, A. J. The System KOH-K_2CO_3-H_2O at Low Temperatures: I. Phase Equilibria. *Can. J. Chem.* **1958**, *36*, 1064−1069.
(54) Carbonnel, L. The Ternary System of H_2O-KOH-K_2CO_3 in the Temperature Interval -22° to -30.7 °. *Bull. Soc. Chim. Fr.* **1959**, 1990−1996.
(55) Byzova, E. A. Solubility of Salts in the System K_2CO_3-K_2SO_4-KCl-H_2O at 0, 30, 50, and 70 °. *Russ. J. Inorg. Chem.* **1963**, *8*, 1014−1017.
(56) Fedotieff, P. P. Der Ammoniaksodaprozess vom Standpunkte der Phasenlehre. *Z. Phys. Chem.* **1904**, *49*, 162−188.
(57) Fedotieff, P. P.; Kolossoff, A. Die Dritte Form des Ammoniaksodaverfahrens. *Z. Anorg. Allg. Chem.* **1923**, *130*, 39−46.
(58) Fedotleff, P.; Koltunoff, J. Eine andere Form des Ammoniaksodaverfahrens. *Z. Anorg. Allg. Chem.* **1914**, *85*, 247−260.
(59) Jänecke, E. Über das System H2O, CO2, NH3. *Z. Elektrochem. Angew. Phys. Chem.* **1929**, *35*, 716−728.
(60) Jänecke, E. Über die Löslickeit von Ammonbicarbonat in Wasser bis zum Schmeltzpunkt. *Z. Elektrochem. Angew. Phys. Chem.* **1929**, *35*, 332−334.
(61) Neumann, B.; Domke, R. Die Gleichgewichtsverhältnisse beim Ammoniaksodaprozesse unter Druck. *Z. Elektrochem. Angew. Phys. Chem.* **1928**, *34*, 136−153.
(62) Toporescu, E. Sur la Preparation du Bicarbonate du Sodium. *Compt. Rend.* **1922**, *174*, 870−873.
(63) Toporescu, E. Sur la Preparation du Bicarbonate du Sodium. *Compt. Rend.* **1922**, *175*, 268−270.
(64) Trypuc, M.; Kielkowska, U. Solubility in the NH_4HCO_3+NH_4VO_3+H_2O System. *J. Chem. Eng. Data* **1996**, *41*, 1005−1007.
(65) Volfkovich, S. I.; Belopolskii, A. P.; Lebedev, B. A. Utilization of Natural Sodium Sulfate for Manufacturing Soda Ash and Ammonium Sulfate. *Zh. Prikl. Khim.* **1931**, *4*, 582−606.
(66) Hartono, A.; Saeed, M.; Kim, I.; Svendsen, H. F. Protonation Constant (pK_a) of MDEA in Water as Function of Temperature and Ionic Strength. *Energy Procedia* **2014**, *63*, 1122−1128.
(67) Tagiuri, A.; Mohamedali, M.; Henni, A. Dissociation Constant (pK_a) and Thermodynamic Properties of Some Tertiary and Cyclic Amines from (298 to 333) K. *J. Chem. Eng. Data* **2015**, *61*, 247−254.
(68) Hyde, A. M.; Zultanski, S. L.; Waldman, J. H.; Zhong, Y.-L.; Shevlin, M.; Peng, F. General Principles and Strategies for Salting-Out Informed by the Hofmeister Series. *Org. Process Res. Dev.* **2017**, *21*, 1355−1370.
(69) Nemati-Kande, E.; Shekaari, H. Salting-out Effect of Sodium, Potassium, Carbonate, Sulfite, Tartrate and Thiosulfate Ions on Aqueous Mixtures of Acetonitrile or 1-Methyl-2-pyrrolidone: A Liquid−Liquid Equilibrium Study. *Fluid Phase Equilib.* **2013**, *360*, 357−366.
(70) Grover, P. K.; Ryall, R. L. Critical Appraisal of Salting-Out and Its Implications for Chemical and Biological Sciences. *Chem. Rev.* **2005**, *105*, 1−10.
(71) Marcus, Y. Effect of Ions on the Structure of Water: Structure Making and Breaking. *Chem. Rev.* **2009**, *109*, 1346−1370.

https://doi.org/10.1021/acs.jced.1c00144
J. Chem. Eng. Data XXXX, XXX, XXX−XXX